A Topological Investigation of the Nonlinear Optical Compound: Iodoform Octasulfur

David J. Wolstenholme,* Katherine N. Robertson, Eduardo Mesa Gonzalez, and T. Stanley Cameron

Department of Chemistry, Dalhousie University, Halifax, Nova Scotia, Canada, B3H 4J3

Received: July 4, 2006; In Final Form: August 29, 2006

The crystal structure of the nonlinear optical material, iodoform octasulfur ($CHI_3 \cdot (S_8)_3$), in the polar space group *R*3*m*, has been shown to contain three unique S···I and several S···S close contacts (≤ 4.0 Å), that fall well below the sum of the van der Waals radii of the two atoms concerned. These interactions have all been characterized topologically following the multipole refinement of the crystal structure of iodoform octasulfur. The natures of the possible charge transfer (S···I) and electrostatic (S···S) interactions in this molecule have been investigated based on charge density studies. The properties of the electron density at the bond critical points provide a tool for determining which of the sulfur or iodine atom acts as the donor and which acts as the acceptor in each of the possible S···I charge-transfer interactions present in this molecule. This all leads to a better understanding of the donor/acceptor nature for both types of atoms in charge-transfer complexes of inorganic nonlinear optical materials. The analysis of the structure of iodoform octasulfur has also provided new insight into the relationship between charge density studies and VSEPR theory.

Introduction

A number of crystal adducts formed from halogen and halide compounds (Br_2, I_2, haloforms, organic halides) acting as electron acceptors, and molecules containing chalcogen atoms acting as electron donors, have been studied using many different techniques including X-ray crystallography.[1−6] It has previously been shown that, in addition to hydrogen bonds, crystals can assemble through the use of other relevant intermolecular interactions such as halogen bonds and charge-transfer interactions.[7−11] Polar (non-centrosymmetric) crystals that contain the latter form of intermolecular interaction are of interest because of their nonlinear optical (NLO) properties. Studies have shown that the strength of the charge transfer between halogens and molecular sulfur enhances the polarizability of such interactions. This results in a large contribution to the quadratic susceptibility, which in turn affects the optical properties of the molecule.[4] Few electron density studies have been carried out for the purpose of fully characterizing the properties of NLO type compounds. The iodoform octasulfur molecule seemed ideally suited for a full topological analysis of its intermolecular interactions through the use of the theory of Atoms in Molecules (AIM).

The theory of AIM has been applied both experimentally and theoretically to a wide variety of structures containing many different types of intermolecular interactions.[6,12,13] This theory states that in a bound equilibrium molecular state, the nuclei of the bonded atoms are linked by a line in which the electron density is a maximum with respect to any neighboring lines, and is referred to as a bond path (BP).[14] Along this BP a minimum in the electron density can be found, which signifies a gateway between the two bonded atoms. This is referred to as the bond critical point (BCP) and possesses several important features such as the electron density at the BCP (ρ_{cp}) and the Laplacian ($\nabla^2\rho_{cp}$), which can be used to characterize an intermolecular interaction.[15,16] The ρ_{cp} values represent the accumulation of electron density at the BCP. In the case of an open-shell interaction (covalent bond) $\rho_{cp} > 0.5$ eÅ^{-3}, whereas in a closed-shell interaction (hydrogen bond or charge-transfer interaction) $\rho_{cp} < 0.5$ eÅ^{-3}. The $\nabla^2\rho_{cp}$ values represent the concentration or depletion of density at the BCP. In open-shell interactions, the $\nabla^2\rho_{cp}$ has a negative value, which indicates that the density is locally concentrated. In closed-shell interactions, the $\nabla^2\rho_{cp}$ value is positive, which indicates that the density is locally depleted at the BCP.

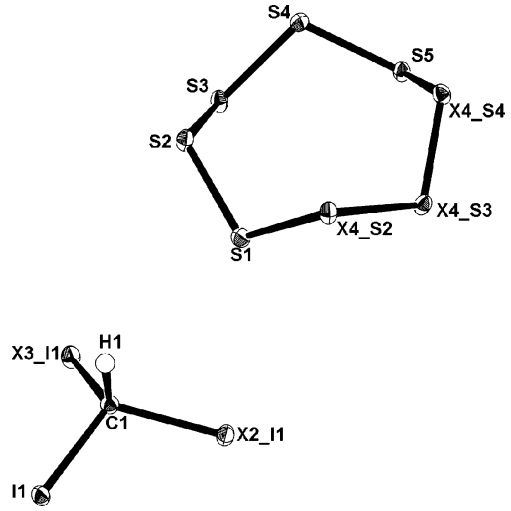

Figure 1. ORTEP diagram (with labels) for atoms of iodoform octasulfur at 93 K with 50% ellipsoid probability.

It has previously been determined that in the linear S···I charge-transfer interaction in iodoform octasulfur (Figure 1) the sulfur atom is the donor atom and that the iodine atom is the acceptor atom.[1−3] However, there are several other S···I intermolecular interactions in the crystal that can possibly also be classified as charge-transfer interactions and these have, so far, not been examined. The present paper characterizes all of

* To whom correspondence should be addressed. Telephone number: 1-(902)-494−3759. Fax number: 1-(902)-494-1310. E-mail: dwolsten@dal.ca.

10.1021/jp064181o CCC: $33.50
Published on Web 11/02/2006

TABLE 1: Experimental X-ray Data

compound formula	HCI_3S_{24}
crystal size (mm)	0.12 × 0.12 × 0.12
formula weight (g/mol)	1163.17
space group	*R*3*m* (#160)
a (Å)	24.317(5)
b (Å)	24.317(5)
c (Å)	4.377(1)
γ (deg)	120.00
V (Å^3)	2241.1(9)
Z	3
μ (cm^{-1})	48.16
D_c (g/cm^3)	2.585
F(000)	1650.00
reflections collected	55303
reflections (multipole)	7495
R(F)	2.23%
GOF	1.3438
no. of parameters (multipole)	199
collection ranges	$-29 \le h \le 63$ $-63 \le k \le 58$ $-8 \le l \le 8$
maximum resolution (2θ)	137.7
Flack parameter	−0.010(6)

the inter/intramolecular interactions (S···I, S···S, I···I, and I···H) present in the iodoform octasulfur molecule based on the properties of the electron density at the BCP. From these results the donor and acceptor atoms in each of the three possible S···I charge-transfer interactions can be determined and compared with the appropriate VSEPR models.

Experimental Section

Needle shaped crystals of iodoform octasulfur were obtained through the evaporation of a 1:3 mixture of iodoform and rock sulfur in carbon disulfide for several days. A perfect light-yellow block, cut from the needle-shaped crystal of CHI_3S_{24}, had approximate dimensions of 0.12 × 0.12 × 0.12 mm. This was mounted on the end of a Lindemann glass capillary, since a tube has a greater resistance to vibration than a fiber of the same cross section. All measurements were made on a Rigaku Saturn CCD area detector with graphite monochromated Mo−Kα radiation. The crystal data for the X-ray diffraction experiment can be found in Table 1. The data were collected at a temperature of −160 ± 1 °C to a maximum 2θ value of 137.7°. A total of 2493 oscillation images were collected using a number of different sweeps (supplementary data). The crystal-to-detector distance was measured to be 39.56 mm. The data collection was monitored and reduced with CrystalClear software,[17] while sorting, scaling, and merging of the intensities were performed with Sortav[18] as included in the WinGX software package.[19] The structure was solved by direct methods and expanded using Fourier techniques using the CrystalStructure software package.[20] All non-hydrogen atoms were refined anisotropically and the hydrogen atoms were refined isotropically. The final cycle of full-matrix least-squares was refined on F and was based on 7495 unique reflection and 53 variables. This refinement converged with unweighted and weighted agreement factors of 2.4% and 2.6% respectively. The final maximum and minimum peaks in the difference Fourier map corresponded to 2.89 and −2.17 eÅ^{-3}, respectively. All calculations were performed using the CrystalStructure crystallographic software package except for the refinements, which were performed using a SHELXL interface.[21] All of the molecular thermal ellipsoid plots were generated using the ORTEP-3 program.[22] The CIF file was deposited in the Cambridge Crystallographic Data Centre. (CCDC 611177 contains the supplementary crystallographic data for this paper. These data can be obtained free of charge via www.ccdc.cam.ac.uk/data_request/cif, or by e-mailing data_request@ccdc.cam.ac.uk, or by contacting The Cambridge Crystallographic Data Centre, 12 Union Road, CB2 1EZ, U.K.; fax: +44 1223 336033.)

Multipole Refinement. The experimental measurements and analysis of the charge density for the iodoform octasulfur crystal have been achieved through the use of high-resolution X-ray diffraction data collected at low temperature. The charge density of this compound was then evaluated through the interpretation of its electron density. The method used to obtain the electron density was the multipole expansion, which incorporates the Hansen-Coppens Model,[23] and can be expressed by the following equation:

$$\rho(\mathbf{r}) = P_c\,\rho_{core}(\mathbf{r}) + P_v\,\kappa^3\,\rho_{valence}(\kappa\mathbf{r}) + \sum_{l=0}^{l_{max}} \kappa'^3\,R_l(\kappa'\mathbf{r}) \sum_{m=0}^{l}\sum P_{lm\pm} d_{lm\pm}(\theta,\varphi) \quad (1)$$

where ρ_{core} and $\rho_{valence}$ are spherically averaged Hartree−Fock core and valence densities, $d_{lm\pm}$ represents spherical harmonic angular functions, R_l is the radial function, κ and κ' are the expansion−contraction parameters, and P_v and $P_{lm\pm}$ represent the population parameters.

The multipole refinements were carried out with the module XDLSM incorporated in the software package XD.[24] The residual bonding density not modeled in the conventional spherical refinement was taken into account in the multipole refinement. The scattering factors used in the multipole refinement were those derived from Bunge et al.[25] for all atoms. The single-ξ functions are taken from Clementi, Roetti, and Raimondi[26,27] wave functions for the iodine atoms. The least-squares refinement involved the minimization of the $\sum w(|F_0|^2 - K|F_c|^2)^2$ function for all reflections with $I > 3\sigma$. The multipole expansion was applied up to the hexadecapole level ($l_{max} = 4$) for all of the heavy atoms except carbon, where it was applied up to the octapole level ($l_{max} = 3$) and up to the dipole level ($l_{max} = 1$) for the hydrogen atom. Separate κ and κ' parameters were employed for all the heavy atoms throughout the multipole refinement. The expansion/contraction parameters of the hydrogen atom were left fixed at the default XDLSM value of 1.2. To determine accurate positional and thermal parameters for the heavy atoms, a high order ($\sin\theta/\lambda \ge 0.6$) refinement was performed. A low order ($\sin\theta/\lambda \le 0.6$) refinement was performed in order to obtain accurate thermal parameters for the hydrogen atom. The C−H bond length was then set to the reported electron diffraction distance of a similar compound for the rest of the multipole refinement (C−H = 1.11 Å).[28] The charge neutrality constraint was applied throughout the multipole refinement in order to achieve an overall neutral molecule. The multipole refinement strategy used was as follows: in five separate stages $P_{monopole} - P_{hexadecapole}$ were refined for all heavy atoms; then κ was refined for all heavy atoms, followed by κ' for all heavy atoms. Finally xyz and U_{ij} values were refined for all heavy atoms, and in the last step everything was refined together except κ'. The scale factor and a type I extinction parameter were refined throughout the refinement. This procedure was cycled through until convergence was achieved. A chemical equivalency constraint was applied to both [S(2), S(3), S(4)] and [S(1), S(5)] for the first two cycles of the multipole refinement. These constraints were applied in order to obtain reasonable monopole populations for the sulfur atoms. In the remainder of the refinement cycles these monopole populations were fixed to the appropriate values, while the multipole

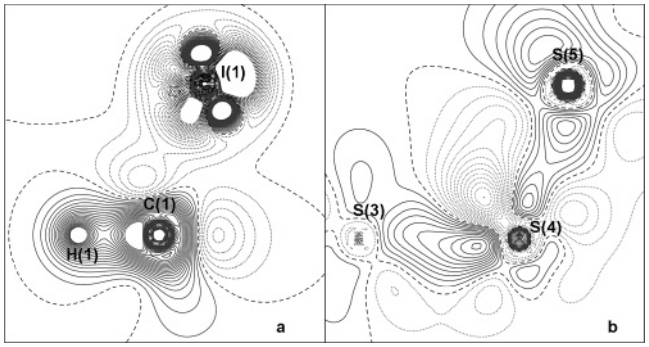

Figure 2. Static deformation maps with positive contours as solid lines, negative contours as dotted lines, and the zero contour line as dashes. (a) H1−C1−I1 plane with contour intervals of 0.05 e Å^{-3}, (b) S3−S4−S5 plane with contour intervals of 0.05 eÅ^{-3}.

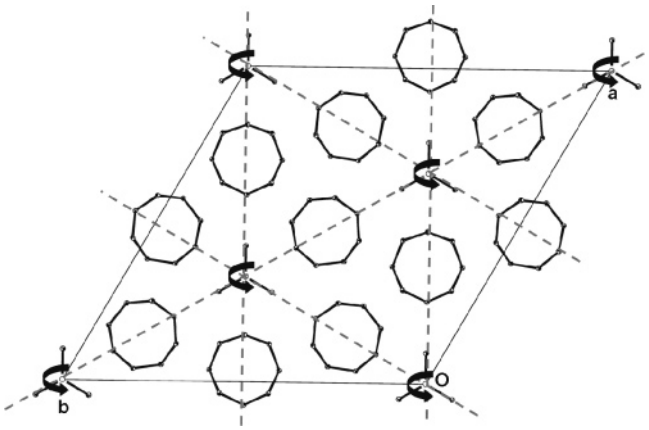

Figure 3. Packing diagram of the iodoform octasulfur adduct in the *ab* plane. The dashed lines represent the mirror plane symmetry, and the arrows represent the 3-fold rotation axis.

populations were allowed to refine freely. The hydrogen atom parameters were left fixed due to difficulties in modeling the multipole parameters of this atom. The difference mean square displacement amplitudes (DMSDA) for all bonds were within the Hirshfeld limits, except C(1)−I(1) which was somewhat higher than the expected value (0.0015). The good quality of the final model is illustrated in the maps of Figure 2, which show the static deformation density of iodoform octasulfur in chosen planes of the molecule. The XDPROP program incorporated into the XD package[24] was then used to determine the total electron density, $\rho(\mathbf{r})$, the Laplacian ($\nabla^2\rho(\mathbf{r})$), and the ellipticity of all the relevant inter/intramolecular interactions present in the molecule. All static, residual, dynamic, and deformation maps were produced using the XDGRAPH option in the XD package.[24] The final atomic coordinates, thermal parameters, and bond lengths for the iodoform octasulfur molecule are provided as Supporting Information.

Results and Discussion

The iodoform octasulfur complex crystallizes in the *R*3*m* space group #160 (Table 1), which contains three perpendicular mirror planes which intersect at the 3-fold rotation axis. Figures 3 and 4 are drawn projected onto the *ab* plane so that this 3-fold axis can be considered as a vertical axis. The iodoform molecule therefore aligns with the C−H bond along the trigonal axis and with the iodine atoms on each of the three vertical mirror planes. Each iodoform molecule is surrounded by three octasulfur molecules, and each molecule lies across one vertical mirror plane. This means that there are only eight unique atoms present in the molecule (C1, H1, I1, S1, S2, S3, S4, and S5), with S1 and S5 on the mirror plane, and the rest of the S_8 ring being generated by the mirror. The remaining two symmetry-related iodine atoms are produced through the use of the 3-fold rotation axis. Each, of course, has its own 'attached' S_8 ring to produce the full (CHI_3·(S_8)$_3$) structure (Figure 3).

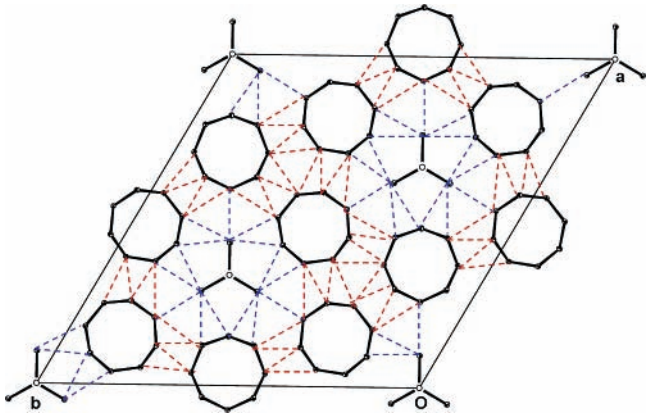

Figure 4. Packing diagram of the iodoform octasulfur adduct in the *ab* plane. The blue dashed lines represent all the intermolecular S···I interactions. The red dashed lines represent all the intermolecular S···S interactions.

All the internuclear distances and bond angles for the iodoform and octasulfur are consistent with those previously observed for this adduct.[27] The C−I and C−H internuclear distances are 2.1508(8) and 1.11 Å, respectively, with an H−C−I bond angle of 106.97(7)°, which is consistent with the expected tetrahedral geometry of the carbon atom.[28,29] The S1−S2, S2−S3, S3−S4, and S4−S5 internuclear distances are 2.0524(5), 2.0587(4), 2.0501(3), and 2.0551(4) Å, respectively. The S1−S2−S3, S2−S3−S4, S3−S4−S5, S2−S1···X4_S2, and S4−S5···X4_S4 bond angles are 107.90(2), 108.01(2), 107.72(2), 107.43(2), and 105.83(2)°, respectively. This octasulfur geometry is consistent with the free octasulfur molecule though it is slightly distorted.[30] The packing of this complex in the unit cell results in a number of short (<4.0 Å) intermolecular interactions (Figure 4). Each iodine atom is closely surrounded by five sulfur atoms belonging to different octasulfur molecules. The shortest intermolecular S···I contact (3.5152(2) Å) is between S5 and I1, with a C−I···S bond angle of 177.13(7)°. There are only two other unique intermolecular S···I contacts, which have internuclear distances of 3.7678(4) (S1···I1) and 3.8279(2) Å (S2···I1) and bond angles of 80.91(3) and 121.95(2)° respectively. All three of these intermolecular interactions are consistent with possible charge-transfer interactions. In addition to the three unique S···I interactions the complex also contains at least eight unique S···S intermolecular interactions that help to stabilize the crystal. The internuclear distances for these interactions range between 3.3319(4) and 4.0119(4) Å, and all appear to be electrostatic (van der Waals interactions) in nature. Finally, the internuclear distances for the I···I and I···H interactions are 4.3765(2) and 3.3480(5) Å, respectively, which are consistent with weak van der Waals interactions.

The experimental topological parameters used to characterize all the intra/intermolecular interactions along with the xyz and translations of the symmetry-related molecules are given in Tables 2 and 3. The first criterion for the identification of any bond is the location of a consistent BP and BCP. Each of the C−H, C−I, S−S bonds, as well as the S··I, S···S, I···I, and I···H intermolecular interactions in the iodoform octasulfur complex has a consistent BP and BCP (Figure 5). The bond path length (R_{ij}) for the C−I bond is 2.152 Å and those of the

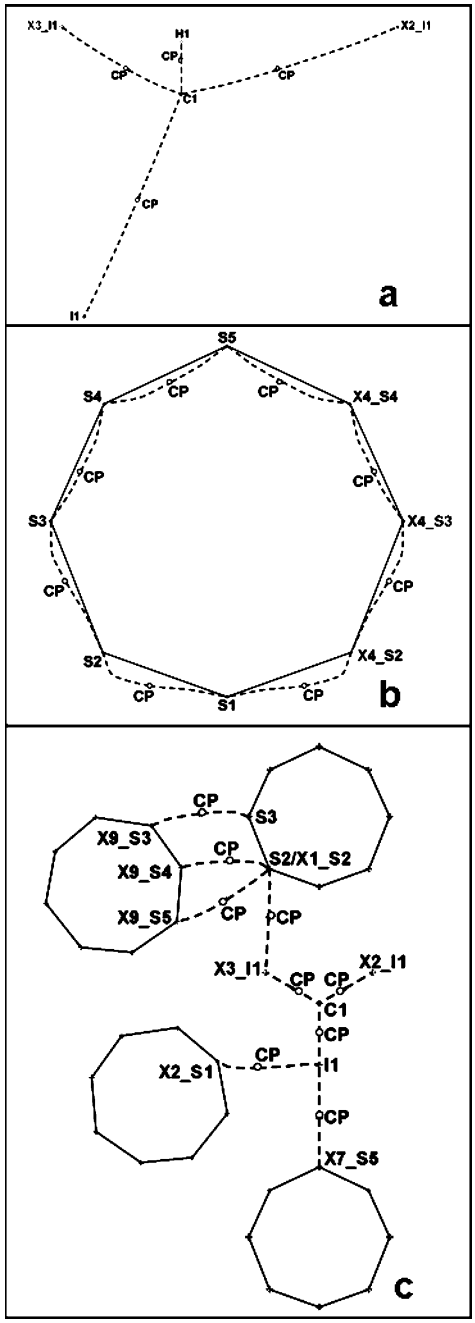

Figure 5. (a) Bond path character in the iodoform portion of the complex showing the critical point location along the C−I and C−H bonds (dashed lines). (b) Bond path character in the octasulfur portion of the complex showing the critical point location along the S−S bonds (dashed lines). (c) Bond path character in the iodoform octasulfur complex showing the critical point location along the S···I and S···S interactions (dashed lines).

S−S bonds range from 2.058 to 2.084 Å. The intermolecular S···I and S···S interactions all have R_{ij} values that fall between 3.356 and 4.013 Å. The intermolecular I···I and I···H interactions have R_{ij} values of 4.3766 and 3.3511 Å. The ρ_{cp} values for both the C−H and C−I bonds in the iodoform portion of this adduct are 1.93 and 0.68 eÅ^{-3}. Interestingly, the ρ_{cp} value for the C−I bond is found at the lower limit of the covalent bond region. The ρ_{cp} values for the S−S bonds all fall between 1.02 and 1.12 eÅ^{-3}, which are well within the range for covalent bonds. Thus, the topological parameters for the regular covalent bonds all fall within the expected range. The S···I and S···S intermolecular interactions have small ρ_{cp} values that range from 0.053 to 0.135 eÅ^{-3} and 0.03 to 0.086 eÅ^{-3}, respectively (Table 3), which are characteristic of weak electrostatic interactions. The I···I and I···H interactions are also characteristic of van der Waals interactions with ρ_{cp} values of 0.054 and 0.051 eÅ^{-3}, respectively. The Laplacian values, $\nabla^2\rho_{cp}$, for the C−H and C−I bonds are −14.140 and 0.166 eÅ^{-5}. The positive value for $\nabla^2\rho_{cp}$ of the C−I bond is indicative of a closed-shell interaction. This has previously been shown to occur for C−I bonds in the study of 1,4-diiodotetrafluorobenzene.[6] The $\nabla^2\rho_{cp}$ values for all the S−S bonds fall between −0.302 to −3.994 eÅ^{-5}, which are characteristic of covalent bonds. The intermolecular interactions have $\nabla^2\rho_{cp}$ values that are small and positive (Table 3), which are again characteristic of closed-shell interactions (charge transfer or van der Waals). The $\nabla^2\rho_{cp}$ values for the S···I interactions range between 0.451 and 0.823 eÅ^{-5}, while the S···S interactions have values between 0.302 and 0.837 eÅ^{-5}. The I···I and I···H interactions also have $\nabla^2\rho_{cp}$ values characteristic of closed-shell interactions (0.320 and 0.422 eÅ^{-5}). The $\nabla^2\rho_{cp}$ maps showing the depletion of electron density at the BCP for an S···I interaction, an S···S interaction, and the C−I bonds are shown in Figure 6.

Chemical bonds and intermolecular interactions can also be characterized through the use of the local electronic energy densities.[31] The potential energy density (V_{cp}), the kinetic energy density (G_{cp}), and the total energy density (H_{cp}) at the BCP can be estimated within the Abramov approximations as shown in the following three equations:[32]

$$G_{cp} = (3/10)\,(3\pi^2)^{2/3}\,\rho^{5/3}{}_{cp} + (1/6)\,\nabla^2\rho_{cp} \qquad (2)$$

$$V_{cp} = (h^2/4m)\,\nabla^2\rho_{cp} - 2G_{cp} \qquad (3)$$

$$H_{cp} = G_{cp} + V_{cp} \qquad (4)$$

It should be noted that the Abramov approximation greatly overestimates both V_{cp} and G_{cp} magnitudes for covalent bonds. However, these errors are compensated for in the calculation of H_{cp} and $|V_{cp}|/G_{cp}$.[6]

Recently, a classification scheme for atomic interactions was proposed based on the properties of the electron density at the BCP.[33] Interactions that are best classified as pure closed-shell (region I) were determined to have $\nabla^2\rho_{cp}$ values > 0 and H_{cp} values > 0. Those that are transit closed-shell (region II) have $\nabla^2\rho_{cp}$ values > 0 and H_{cp} values < 0 and purely open-shell interactions (region III) have $\nabla^2\rho_{cp}$ values < 0 and H_{cp} values < 0. The boundaries between regions I, II, and III are defined by $H_{cp} = 0$ ($|V_{cp}|/G_{cp} = 1$) and $\nabla^2\rho_{cp}$ values equal to zero. The H_{cp} values for the C−H/C−I bonds are −1065.12 and −163.40 kJ mol^{-1} bohr^{-3}, which along with their $\nabla^2\rho_{cp}$ values seems to indicate that the C−H bond is covalent (region III) and the C−I bond is transit closed-shell (region II). The S−S bonds in the octasulfur ring have H_{cp} values that range from −333.91 to −411.89 kJ mol^{-1} bohr^{-3}. Since all the S−S bonds have negative $\nabla^2\rho_{cp}$ values, they can be classified as covalent bonds (region III). The intermolecular S···I interactions between I(1) and S(1)/S(2) both have positive $\nabla^2\rho_{cp}$ values along with H_{cp} values of 1.7549 and 0.5503 kJ mol^{-1} bohr^{-3} respectively. This indicates that these interactions are purely closed-shell in nature. The strong linear S···I interaction between I(1) and S(5) has a positive $\nabla^2\rho_{cp}$ value and a negative H_{cp} value of −3.6426 kJ mol^{-1} bohr^{-3}, which means this interaction is best classified as transit closed-shell. All the intermolecular S···S interactions possess positive $\nabla^2\rho_{cp}$ values and positive H_{cp} values that are between 1.8049 and 2.7012 kJ mol^{-1} bohr^{-3}, which indicates

TABLE 2: Properties of the Electron Density at the BCP for All the Intramolecular Interactions

interaction	ρ_{cp} (e Å^{-3})	$\nabla^2\rho_{cp}$ (e Å^{-5})	R_{ij} (Å)	d1 (A-CP) (Å)	d2 (CP-B) (Å)	Λ_A	Λ_B	$\lvert V_{cp}\rvert/G_{cp}$	H_{cp} (kJ mol^{-1} bohr^{-3})
C(1)−H(1)	1.931	−14.14	1.11	0.7529	0.3571	0.407	0.298	2.566	−1065.120
C(1)−I(1)	0.681	0.166	2.1519	1.0788	1.0731	0.583	0.542	1.973	−163.398
S(1)−S(2)	1.049	−0.302	2.0843	1.0803	1.0040	0.584	0.543	2.025	−341.545
S(2)−S(3)	1.018	−1.281	2.0589	1.0266	1.0323	0.555	0.558	2.117	−333.911
S(3)−S(4)	1.109	−1.418	2.0583	0.9908	1.0676	0.536	0.577	2.112	−384.587
S(4)−S(5)	1.116	−3.994	2.0919	1.1001	0.9918	0.595	0.536	2.359	−411.891

TABLE 3: Properties of the Electron Density at the BCP for All the Intermolecular Interactions

interaction	ρ_{cp} (e Å^{-3})	$\nabla^2\rho_{cp}$ (e Å^{-5})	R_{ij} (Å)	d1 (A-CP) (Å)	d2 (CP-B) (Å)	Λ_A	Λ_B	$\lvert V_{cp}\rvert/G_{cp}$	H_{cp} (kJ mol^{-1} bohr^{-3})	bond energies (kJ mol^{-1} bohr^{-3})
I(1)−X4_I(1)	0.054	0.320	4.3766	2.1896	2.1870	1.106	1.105	0.940	0.492	−3.8661
I(1)−X1_H(1)	0.051	0.422	3.3511	2.1315	1.2197	1.077	1.016	0.834	1.637	−4.1097
I(1)−X2_S(1)	0.053	0.451	3.8398	2.1331	1.7061	1.077	0.923	0.833	1.755	−4.3867
I(1)−X2^1_S(2)	0.073	0.500	3.8282	2.0421	1.7861	1.031	0.965	0.957	0.550	−6.2586
I(1)−X7_S(5)	0.135	0.823	3.5162	1.8346	1.6815	0.927	0.909	1.140	−3.643	−14.8500
S(1)−X1_S(2)	0.040	0.428	3.8413	2.0002	1.8411	1.081	0.995	0.738	2.422	−3.4064
S(2)−X1^1_S(3)	0.030	0.302	4.0133	1.9821	2.0312	1.071	1.098	0.713	1.836	−2.2770
S(2)−X9_S(4)	0.048	0.516	3.5080	1.7102	1.7979	0.924	0.972	0.762	2.701	−4.3256
S(2)−X9_S(5)	0.041	0.400	3.6740	1.7667	1.9073	0.955	1.031	0.760	2.106	−3.3408
S(3)−X9_S(3)	0.047	0.497	3.5964	1.7740	1.8225	0.959	0.985	0.763	2.597	−4.1709
S(3)−X1_S(4)	0.050	0.506	3.6775	1.7622	1.9153	0.953	1.035	0.782	2.471	−4.4198
S(3)−X9^1_S(4)	0.086	0.837	3.3556	1.3677	1.7179	0.885	0.929	0.885	2.357	−9.0412
S(4)−X1^1_S(5)	0.045	0.395	3.8852	1.9306	1.9545	1.044	1.056	0.798	1.805	−3.5741

Symmetry

	x,*y*,*z*	TA	TB	TC
X1	+*x*, +*y*, +*z*	0	0	−1
X1^1	+*x*, +*y*, +*z*	0	0	1
X2	−*y*, +*x*−*y*, +*z*	0	0	0
X2^1	−*y*, +*x*−*y*, +*z*	0	0	−1
X4	−*x*+*y*, +*y*, +*z*	0	0	0
X7	2/3+*x*, 1/ 3+*y*, 1/ 3+*z*	−1	−1	−1
X9	2/3−*x*+*y*, 1/3−*x*, 1/ 3+*z*	−1	0	0
X9^1	2/3−*x*+*y*, 1/3−*x*, 1/ 3+*z*	−1	0	−1
X14	1/3−*y*, 2/ 3+*x*−*y*, 2/3+*z*	0	0	−1

that they are purely closed-shell in nature. Finally, the intermolecular I···I and I···H interactions both have positive $\nabla^2\rho_{cp}$ and H_{cp} values (Table 3), which indicate that they are also closed-shell interactions.

The V_{cp} and G_{cp} parameters can be interpreted as the pressures exerted on and by the electrons at the BCP. This indicates that a $|V_{cp}|/G_{cp}$ ratio could be used to determine the nature of a chemical bond. A $|V_{cp}|/G_{cp}$ value less than one indicates a depletion of charge, which in turn indicates a closed-shell interaction. When $|V_{cp}|/G_{cp} > 2$, the interaction is stabilized by a local concentration of charge (open-shell). Finally, when $1 < |V_{cp}|/G_{cp} < 2$, the interaction falls somewhere between an open- and closed-shell interaction and is classified as transit.[33] The $|V_{cp}|/G_{cp}$ ratio is therefore another useful method which can be used to help determine the nature (closed/transit/open) for all chemical bonds and intermolecular interactions in a desired complex. In this work, the experimental ratio $|V_{cp}|/G_{cp}$ for the C−I bond is 1.97, which is consistent with previous experimental and DFT/RHF calculations (1.71 and 1.58) for C−I bonds.[6] This supports the claim that the C−I bond in iodoform is a transit closed-shell interaction. The S−S bonds in the octasulfur portion of the complex have $|V_{cp}|/G_{cp}$ ratios that range from 2.03 to 2.36, all of which fall in the purely shared region. All the intermolecular interactions but one have $|V_{cp}|/G_{cp}$ ratios that range from 0.713 to 0.957 (Table 3), which classifies them as purely closed-shell in nature. The exception to this is the linear X7_S(5)···I(1) interaction, which has a $|V_{cp}|/G_{cp}$ ratio of 1.14 and is consistent with a transit closed-shell interaction.

The octasulfur ring also contains two ring critical points (RCP) located on the mirror plane. The two RCP are to be expected since the crown can be thought of as two four-membered rings, with their planes parallel and with one plane, shifted 45° with respect to the other. Each four-membered ring will therefore have its own ring critical point. The accumulation of electron density at these RCPs is quite small (0.005 and 0.013 eÅ^{-3}). The $\nabla^2\rho(r_{cp})$ at the RCPs are 0.05 and 0.141 eÅ^{-5}, respectively. This shows that there is a slight depletion in the density at these positions.

The octasulfur portion of this adduct helps to stabilize the crystalline state of the molecule by forming several intermolecular S···S interactions. The approximate bond energies associated with closed-shell interactions, including intermolecular S···S interactions, can be calculated through the use of the following relationship.[34]

$$\text{bond energy} = 1/2(V_{cp}) \tag{5}$$

Correlations between the bond energies and R_{ij} values for the S···S interactions suggest a power fit ($y = a \times x^b$) between the two parameters (Figure 7). This shows that the strengths of these intermolecular S···S interactions are proportional to the bond path lengths.

The S(1) atom interacts with X1_S(2) to give a bond energy of −3.4064 kJ mol^{-1} bohr^{-3}. The S(2) atom interacts with three other sulfur atoms from symmetry related molecules (X1^1_S(3), X9_S(4), and X9_S(5)), which give rise to bond energies of −2.6770, −4.3256, and −3.3408 kJ mol^{-1} bohr^{-3} respectively. The S(3) atom forms three other unique S···S intermolecular interactions (S(3)-X9_S(3), S(3)-X1_S(4), and S(3)-X9^1_S(4)). These three interactions have bond energies of −4.1709,

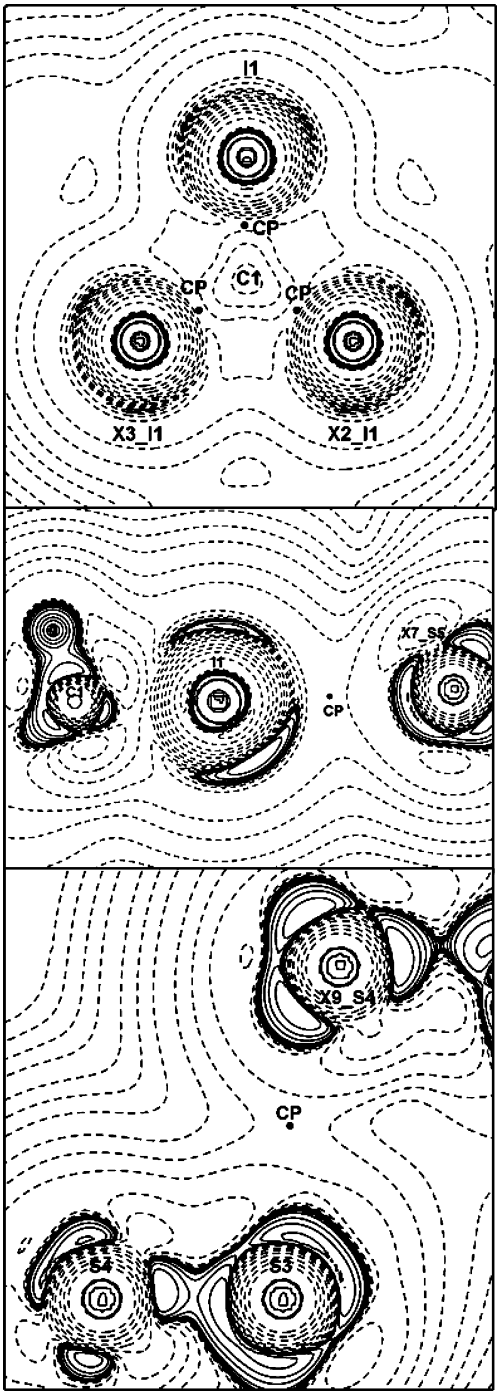

Figure 6. Laplacian maps with positive contours as solid lines, and negative contours as dashed lines (a) I1-X2_I1-X3_I1 plane with contour intervals of 1.0 eÅ^{-5}, (b) C1−I1···X7_S5 plane with contour intervals of 1.0 e Å^{-5}, (c) S4−S3···X9_S4 plane with contour intervals of 1.0 eÅ^{-5}.

−4.4198, and −9.0412 kJ mol^{-1} bohr^{-3}, respectively. Finally, the S(4) atom also interacts with a symmetry related S(5) atom (S(4)-X1^1_S(5)) with a total bond energy of −3.5741 kJ mol^{-1} bohr^{-3}. This indicates that the strongest S···S interaction is between S(3) and X9^1_S(4), and it is equivalent in strength to a weak hydrogen bond. The weakest S···S interaction is between S(2) and X1^1_S(3), and it is equivalent in strength to a weak van der Waals interaction. Thus, a large range of strengths can be observed for these intermolecular S···S interactions. As all five unique sulfur atoms carry a slight positive charge, the interactions are best classified as electrostatic; however, the strong S(3)-X9^1_S(4) interaction warrants further investigation.

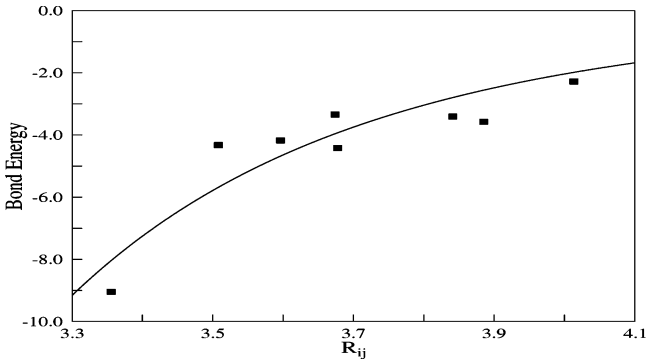

Figure 7. Correlation plot between the overall bond energies (kJ/mol bohr^3) vs the R_{ij} (Å), showing a power fit for all the S···S interactions present in the iodoform octasulfur complex. The R^2 value for this fit is 81.06%, with fitting parameters of a = -1.0×10^5 and $b = -7.811$.

Early studies on the directional preference of S···S interactions has shown that three types of angular approaches occur for S···S interactions in the crystalline state.[35] The interaction from S_i can approach a second sulfur (S_j) atom at roughly 20° to the perpendicular of the plane including S_j and the two atoms bonded to it (type I), or the direction of the S_i···S_j interaction can be roughly along one of the two covalent bonds at S_i. In this case, the S_i···S_j interaction makes an angle close to 90° to the plane of S_i and the two atoms bonded to it (type II).[35] The third type of approach required each of the two angles, to each of the two planes (θ_i,θ_j), to be approximately equal. If both angles are close to 45(±10)°, the interaction is classified as type IIIa. If at least one of the angles is significantly greater than 45°, it can be considered type IIIb.

In the crown sulfur, S(1) and S(5) are predominately involved in S···I interactions. The remaining three sulfur atoms (S(2), S(3), and S(4)) each form three S···S interactions in the range 3.25 to 3.75 Å. Interestingly, each of these three atoms forms one type I/II, one type IIIa, and one type IIIb interaction. The geometry of these S···S interactions are consistent with those previously proposed.[35] However, the two type I/II interactions are the S(3)···X9_S(3) and S(2)···X9_S(4) interactions, where none of the atoms can be distinguished as either electrophiles or nucleophiles.

Since the electronegativity of the sulfur atom (2.58)[36] and the iodine atom (2.66)[36] are relatively similar to one another, the donor and acceptor natures of S···I charge-transfer interactions are difficult to determine. Thus, in all three possible charge-transfer S···I interactions present in the crystal structure of iodoform octasulfur, the nature of both the iodine and sulfur atoms has been examined through VSEPR and the properties of the electron density at the BCP. In charge density studies the location of the BCP or the amount each atom is penetrated by the BCP and can be used to determine whether an atom is a donor or an acceptor. The mutual penetration of two atoms is normally measured with the $\Delta r_A + \Delta r_B$ parameter, where the $\Delta r_{A,B}$ terms represent the gas-phase nonbonding radius ($r^\circ_{A,B}$) of the acceptor/donor atom minus its bonding radius ($r_{A,B}$).[15,16] The gas-phase nonbonding radii used for the sulfur and iodine atoms were 1.85 and 1.98 Å respectively.[37,38] The bonding radius is simply taken as the distance from the donor/acceptor nucleus to the BCP. Another term usually associated with the mutual penetration of the two atoms is the $\Delta r_A - \Delta r_B$ parameter, which if positive indicates that the BCP is closer to the donor (A) and when negative indicates that the BCP is closer to the acceptor (B).[15,16] Both these parameters have thus far only been applied to interactions involving two atoms of approximately the same size. However, when the sizes of the two atoms vary signifi-

cantly, these parameters are no longer valid since the proportion of penetration with respect to the size of the atoms cannot be determined. Since the size of the two atoms involved in these interactions are very different from one another, a variation on the method for determining the location (amount of penetration) of the BCP has been applied instead of the normal $\Delta r_A - \Delta r_B$ criterion used for hydrogen bonding. To account for the differences in size of the two atoms a ratio (Λ_A:Λ_B) has been developed to decide whether the BCP is penetrating further into atom A or B. This is determined through the comparison of the Λ terms in the above ratio. The Λ terms involved in this ratio can be calculated using the following equation:

$$\Lambda_{A \text{ or } B} = r_{A,B}/r^{\circ}_{A,B} \quad (6)$$

When $\Lambda \geq 1$, the gas-phase nonbonding radius is equal to or less than the bonding radius, which indicates that the atom in not being penetrated by the BCP. However, when $\Lambda < 1$ the atom is being penetrated by the BCP since the bonding radius is less than the gas-phase nonbonding radius. When considering the Λ_A:Λ_B ratio, the smaller Λ term indicates that the BCP is closer to that nucleus, which in turn means that this atom is the donor.

There are three unique S···I interactions; one is essentially collinear with the C−I bond axis, a second is at right angles to the bond axis and the third occurs at an intermediate angle. According to VSEPR theory, iodine can be either hexacoordinate or pentacoordinate depending on the number of charge-transfer interactions in which it participates. In this case there are two possibilities. The first possibility is a trigonal bipyrimidal geometry, in which the iodine atom participates in one C−I covalent bond, and has three lone pairs, and one additional charge-transfer interaction. The second possibility is an octahedral geometry, in which one C−I covalent bond, two lone pairs, and two charge-transfer interactions (one with a sulfur donor and one with an iodine donor) are present. The strongest S···I interaction in this complex occurs between X7_S5 and I1 with a nearly linear C1−I1···X7_S5 bond angle of 177.13(7)°. According to VSEPR this is consistent with a charge-transfer interaction, in which the sulfur atom is the donor and the iodine atom is the acceptor. If this is the only charge-transfer interaction occurring between the iodoform and the octasulfur, the iodine atom would be considered a trigonal bipyramidal AX_2E_3 system which is consistent with the nearly linear interaction observed. The Λ ratio for the I1···X7_S5 interaction is 0.927:0.909, which means that the BCP is located relatively closer to the sulfur atom. This agrees with the VSEPR conclusion that the sulfur atom acts as the donor in this interaction. It should also be noted that both atoms are being penetrated by the BCP since the Λ values are below 1.0, which indicates that the distances from the BCP to the nuclei of both the desired atoms are less than their respective gas-phase van der Waals nonbonding radii.

The second S···I interaction in this complex occurs between X2_S1 and I1 and has a C1−I1···X2_S1 bond angle of 80.91(3)°. According to VSEPR this interaction is not quite consistent with a charge-transfer interaction, which would require a C−I···S bond angle of approximately 90°. The Λ ratio for the I1···X2_S1 interaction is 1.077:0.923, which supports the conclusion made by VSEPR. The Λ value for the iodine atom is greater than one, which indicates that the distance from the BCP to the iodine nucleus is greater than the gas-phase van der Waals nonbonding radius. Thus, there is no mutual penetration of the two atoms confirming the absence of a charge-transfer interaction.

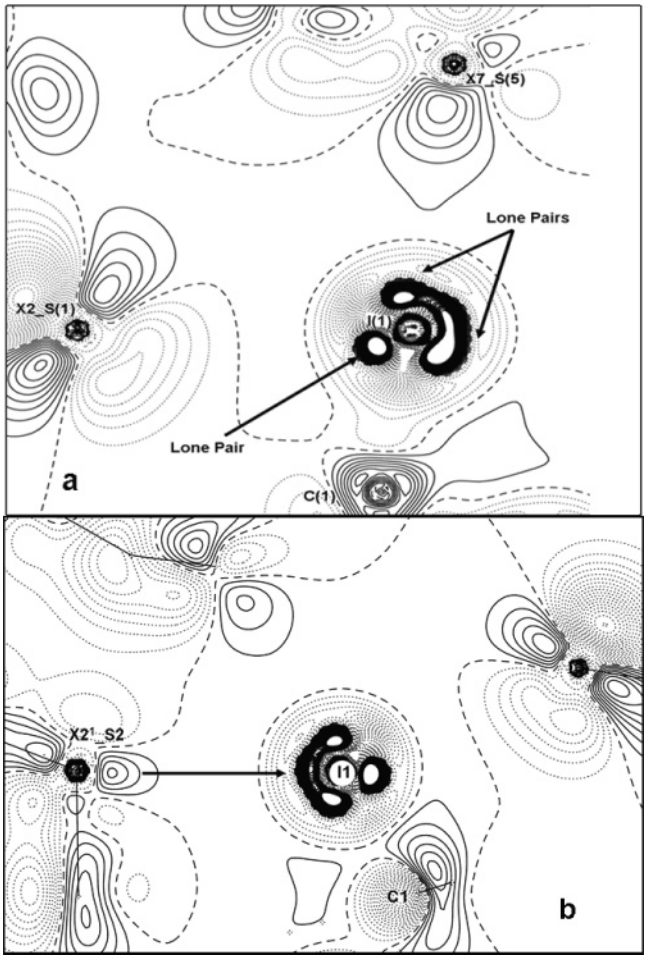

Figure 8. (a) Static deformation map of the iodoform octasulfur in the X2_S(1)···I(1)···X7_S(5) plane, showing the three lone pairs, the C−I bond, and the X7_S(5) charge-transfer interaction. (b) Static deformation map of the iodoform octasulfur in the $X2^1$_S(2)···I1···X3_S(1) plane, showing the interaction between $X2^1$_S(2) and two of the lone pairs. The positive contours are represented as solid lines, negative contours as dotted lines, and the zero contour line as dashes.

The third S···I interaction in this complex occurs between $X2^1$_S2 and I1, and has a C1−I1···$X2^1$_S2 bond angle of 121.95(2)°. According to VSEPR this would be consistent with an AX_4E_2 iodine center. However, the presence of the strong linear charge-transfer interactions and three lone pairs (Figure 8a) indicates that a trigonal bipyrimidal (AX_2E_3) iodine center is present in this complex. The bond angles between X7_S5···I1···$X2^1$_S2 and X2_S1···I1···$X2^1$_S2 are 59.058(6) and 59.215(6)° respectively, which is not consistent with an octahedral geometry. The Λ ratio for I1···X2_S2 is 1.031:0.965, essentially neither donor nor acceptor, with no interpenetration between the two atoms. This suggests that this interaction is electrostatic (van der Waals) in nature rather than a charge-transfer interaction and is occurring through the face of the trigonal bipyrimid, interacting with the two sets of lone pair electrons (Figure 8b).

The properties of the electron density at the BCP can therefore be used to distinguish between charge transfer and purely electrostatic interactions (van der Waals) for these NLO compounds. The first observed difference between the two types of interactions is in the $\rho(r_{cp})$ value. Charge-transfer interactions will have $\rho(r_{cp})$ values greater than 0.1 eÅ^{-3}, whereas purely electrostatic interactions will have a $\rho(r_{cp})$ considerably less than 0.1 eÅ^{-3}. The second difference is in the amount of depletion

of the density at the BCP. Charge-transfer interactions will have $\nabla^2\rho(r_{cp})$ closer to a value of 1.0 eÅ^{-5}, whereas purely electrostatic interactions fall considerably lower ($\sim$0.5 eÅ^{-5}). The final and the most important difference is the mutual penetration of the acceptor and donor atoms. Both the acceptor and donor atoms in charge transfer interactions will be penetrated, whereas purely electrostatic interactions require no mutual penetration.

Conclusion

Experimental charge density studies on the charge-transfer complex of iodoform octasulfur has led to the clear characterization of one S···I charge-transfer interaction, which can be justified using VSEPR theory and which leads to a trigonal bipyramidal geometry at the iodine. Several S···S electrostatic interactions along with two other S···I, an I···I, and an I···H electrostatic interaction have also been characterized based on the properties of the electron density at the BCP. The S(3)···X9^1_S(4) interaction has been shown to be characteristic of a transit closed-shell interaction, which could possibly indicate a different form of intermolecular interaction from the other S···S interactions. The covalent/ionic nature of all the C−I and S−S bonds have also been determined through the use of the H_{cp} and $\nabla^2\rho_{cp}$ analyses, as well as the analysis of the $|V_{cp}|/G_{cp}$ ratio. Several topological differences have been shown to be useful in distinguishing charge-transfer interactions from electrostatic interactions (van der Waals). Finally, these interactions have been shown to play an important role in the stability of the crystalline state of iodoform octasulfur.

Acknowledgment. We are indebted to Rigaku/MSC, The Woodlands, Texas, for provision of the low-temperature data collection facilities during a Sabbatical Leave Fellowship to T.S.C. We thank the Natural Sciences and Engineering Research Council of Canada for Financial support. We also thank Dr. O. Knop and Dr. J. Pincock for helpful discussions on the topic.

Supporting Information Available: The final atomic coordinates, anisotropic displacement parameters, bond lengths, multipole population coefficients, and κ and κ' values obtained from the multipole refinement. This material is available free of charge via the Internet at http:// pubs.acs.org.

References and Notes

(1) Bjorvatten, T. *Acta Chem. Scand.* **1962**, *16*, 749−754.
(2) Bjorvatten, T.; Hassel, O.; Lindheim, A. *Acta Chem. Scand.* **1963**, *17*, 689−702.
(3) Dahl, T.; Hassel, O. *Acta Chem. Scand.* **1970**, *24*, 377.
(4) Munn, R. W.; Kelly, J. F.; Aicken, F. M. *Chem. Phys*. **1999**, *245*, 227−241.
(5) Kelly, J. F.; Krausz, E. R.; Samoc, A.; Samoc, M.; Willis, A. *Aust. J. Chem*. **2002**, *55*, 709−714.
(6) Bianchi, R.; Forni, A.; Pilati; T. *Acta Crystallogr*. **2004**, *B60*, 559−568.
(7) Desiraju, G. R.; Harlow, R. L. *J. Am. Chem. Soc*. **1989**, *111*, 6757−6764.
(8) Burling, F. T.; Goldstein, B. M. *J. Am. Chem. Soc.* **1992**, *114*, 2313−2320.
(9) Desiraju, G. R. *J. Chem. Soc., Chem. Commun*. **1997**, 1475−1481.
(10) Allen, F. H.; Baalham, C. A.; Lommerse, J. P. M.; Raithby, P. R. *Acta Crystallogr*. **1998**, *B54*, 320−329.
(11) Choudhury, A. R.; Urs, U. K. ; Guru Row: T. N.; Nagarajan, K. *J. Mol. Struct.* **2002**, *605*, 71−77.
(12) Munshi, P.; Row: T. N. G. *J. Phys. Chem. A* **2005**, *109*, 659−672.
(13) Chopra D.; Row: T. N. G. *Crystal Growth Des.* **2005**, *5*, 1679−1681.
(14) Bader, R. F. W. *Atoms in Molecules: A Quantum Theory*; Oxford University Press: Oxford, U. K., 1990.
(15) Koch, U.; Popelier, P. *J. Phys. Chem.* **1995**, *99*, 9747.
(16) Popelier, P. *Atoms in Molecules. An Introduction*; Prentice Hall; U.K.; 2000.
(17) Crystal Clear: Rigaku Corporation, 1999. CrystalClear Software User's Guide, Molecular Structure Corporation, 2000. Pflugrath, J. W. *Acta Crystallogr*. **1999**, *D55*, 1718−1725.
(18) Blessing, R. H. *Crystallogr. Rev*. **1987**, 1, 3−58.
(19) Farrugia, L. J.; WinGX (Version 1.64.05) *J. Appl. Crystallogr*. **1999**, *32*, 837−838.
(20) *CrystalStructure 3.6.0*: Crystal Structure Analysis Package, Rigaku and Rigaku/MSC (2000−2004), 9009 New Trails Dr., The Woodlands, TX 77381.
(21) Sheldrick, G. M.; SHELXS97 AND SHELXL97 programs for crystal structure refinement; University of Gottengen; Germany, 1997.
(22) Farrugia, L. J. ORTEP-3. *J. Appl. Crystallogr*. **1997**, *30*, 565.
(23) Coppens, P. *X-ray Charge Densities and Chemical Bonding*; Oxford University Press Inc.; Oxford, U. K., 1997.
(24) Koritsanszky, T. S.; Howard, S.; Macchi, P.; Gatti, C.; Farrugia, L. J.; Mallinson, P. R.; Volkov, A.; Su, Z.; Richter, T.; Hansen, N. K.; XD (version 4.10, July 2003), Free University of Berlin, Germany; University of Wales, Cardiff, U.K.; Universita di Milano, U.K.; CNR−ISTM, Milano, U.K.; University of Glasgow, U.K.; State University of New York, Buffalo, U.S.A.; University of Nancy, France, 2003.
(25) Bunge, C. F.; Barrientos, J. A.; Bunge, A. V. *At. Data Nucl. Data Tables* **1993**, *53*, 113−162.
(26) Clementi, E.; Raimondi, D. L. *J. Chem. Phys*. **1963**, *38*, 2686−2689.
(27) Clementi, E.; Roetti, C. *At. Data Nuclear Data Tables* **1974**, *14*, 177−478.
(28) Tamagawa, K.; Kimura, M. *Bull. Chem. Soc. Jpn*. **1979**, *52*, 7.
(29) Bjorvatten, T. *Acta Chem. Scand.* **1962**, *16*, 749−754.
(30) Coppens, P.; Yang, Y. W.; Blessing, R. H.; Cooper, W. F.; Larsen, F. K. *J. Am. Chem.* Soc. **1977**, *99*, 760−766.
(31) Bader, R. F. W.; Beddall, P. M. *J. Phys. Chem.* **1972**, *56*, 3320−3329.
(32) Abramov, Y. A. *Acta Crystallogr*. **1997**, *A53*, 264−272.
(33) Espinosa, E.; Alkorta, I.; Elguero, J.; Molins, E. *J. Chem. Phys.* **2002**, *117*, 12, 5529−5542.
(34) Espinosa, E.; Molins, E.; Lecomte, C. *Chem. Phys. Lett.* **1998**, *285*, 170−173.
(35) Row: T. N. G.; Parthasarathy, R. *J. Am. Chem. Soc.* **1981**, *103*, 477−479.
(36) Suresh, C. H.; Koga, N. *J. Am. Chem. Soc*. **2001**, *124*, 1790−1797.
(37) Bondi, A. *J. Phys. Chem.* **1964**, *68*, 441−451.
(38) Nyburg, S. C.; Faerman, C. H. *Acta Crystallogr*.. **1985**, *B41*, 274−279.